

# FLAF: Focal Line and Feature-constrained Active View Planning for Visual Teach and Repeat

Changfei Fu, Weinan Chen, Wenjun Xu, and Hong Zhang<sup>†</sup>

**Abstract**—This paper presents FLAF, a focal line and feature-constrained active view planning method for tracking failure avoidance in feature-based visual navigation of mobile robots. Our FLAF-based visual navigation is built upon a feature-based visual teach and repeat (VT&R) framework, which supports many robotic applications by teaching a robot to navigate on various paths that cover a significant portion of daily autonomous navigation requirements. However, tracking failure in feature-based visual simultaneous localization and mapping (VSLAM) caused by textureless regions in human-made environments is still limiting VT&R to be adopted in the real world. To address this problem, the proposed view planner is integrated into a feature-based visual SLAM system to build up an active VT&R system that avoids tracking failure. In our system, a pan-tilt unit (PTU)-based active camera is mounted on the mobile robot. Using FLAF, the active camera-based VSLAM operates during the teaching phase to construct a complete path map and in the repeat phase to maintain stable localization. FLAF orients the robot toward more map points to avoid mapping failures during path learning and toward more feature-identifiable map points beneficial for localization while following the learned trajectory. Experiments in real scenarios demonstrate that FLAF outperforms the methods that do not consider feature-identifiability, and our active VT&R system performs well in complex environments by effectively dealing with low-texture regions.

**Index Terms**—VT&R, Active View Planning, Low Texture

## I. INTRODUCTION

Learning to cruise a path while traversing it is a fundamental capability for mobile robots [1]. Considering that humans and vehicles mainly rely on various flexibly fixed paths to repeatedly shuttle between multiple locations, Teach and Repeat (T&R) [2] is an essential technique for robots to learn to navigate the paths that cover a major part of autonomous navigation requirements. This technique can support many robotic applications, such as household robots traveling between different rooms [3], delivery robots taking goods from the logistics center to the target building [4], and autonomous buses following a mostly fixed trajectory.

As a type of natural visual sensor, monocular cameras are cost-effective, energy-efficient, and versatile, making them suitable for a wide range of environments and applications. The T&R approaches that predominantly utilize visual sensors

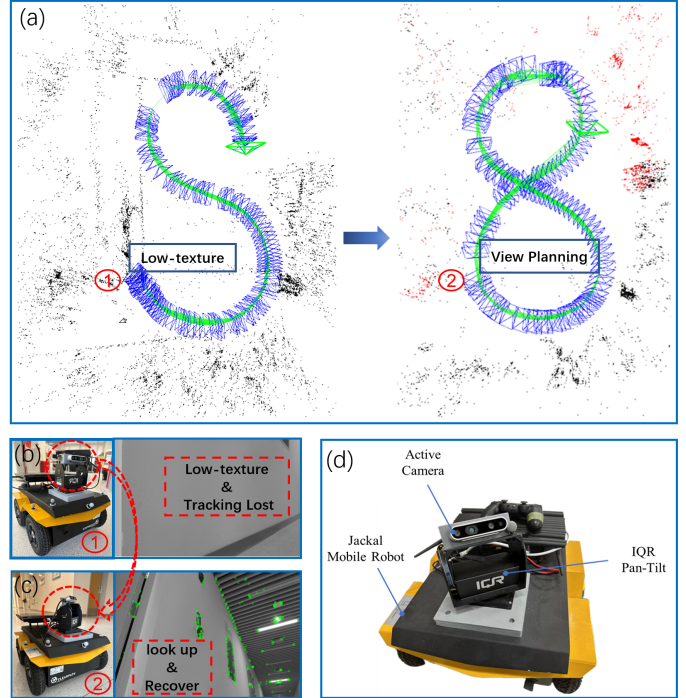


Fig. 1. The left side of Fig. (a) illustrates the failure of the feature-based VT&R system to learn a complete path due to a low-texture region. The corresponding orientation and view of the passive camera are depicted in Fig. (b). In contrast, with our FLAF method and an active camera, the VT&R system successfully navigates this challenging area by directing the camera toward feature-rich regions, as shown in Fig. (c). Fig. (d) presents our mobile robot equipped with an active camera.

are referred to as Visual Teach and Repeat (VT&R) [1], which is a significant motivation of the research in visual simultaneous localization and mapping (VSLAM) [5]. Our active VT&R system integrates a pan-tilt unit (PTU)-based active camera with feature-based VSLAM (see Fig. 1). During the teaching phase, the mobile robot reconstructs the surrounding landmarks while traversing a path under guidance [6]. In the repeat phase, the previously saved path map is reloaded to localize the robot for navigating the taught trajectory.

Although feature-based VSLAM systems [7], [8] achieve impressive robustness and stability in large indoor and outdoor environments [9], they all suffer from the view angle-dependent affine change [10] of features, and the map for real-time localization are usually too sparse for other complex applications [11]. Fortunately, the limited view-angle invariance of features and sparse map for reliable localization is enough for path following in VT&R. In this work, we achieved a high success rate and reliability in passive VT&R

<sup>†</sup>Corresponding author (hzhang@sustech.edu.cn)

Changfei Fu and Hong Zhang are with the Shenzhen Key Laboratory of Robotics and Computer Vision, Southern University of Science and Technology (SUSTech), and the Department of Electrical and Electronic Engineering, SUSTech, Shenzhen, China. Changfei Fu and Wenjun Xu are also with the Peng Cheng National Laboratory, Shenzhen, China. Weinan Chen is with the Biomimetic and Intelligent Robotics Lab, Guangdong University of Technology, Guangzhou, China. This work was supported by the Shenzhen Key Laboratory of Robotics and Computer Vision (ZDSYS20220330160557001).

(using a fixed camera) with feature-based monocular VSLAM. However, textureless regions in human-made environments are still limiting VSLAM and VT&R to be used in the real world. To solve this problem, existing active SLAM works mostly choose to change the robot trajectory, which is not suitable for VT&R [12]. In order to use an active camera to actively select informative views without interfering in the T&R trajectory, our work focuses on designing an active view planning method with active camera-based VSLAM suitable for VT&R.

Our motivation is to design a feature-based VT&R system coupled with active view planning for tracking failure avoidance. Previous active camera-based VSLAM systems [14]–[16] have primarily focused on maintaining stable localization during the mapping process but have not demonstrated how to effectively reuse the map with active view planning for navigation tasks. The key difference between mapping and reusing the map is that there are more choices of map points when the map is complete during navigation, compared to the mapping process when the active camera has no choice but to orient to the newly built map points. As shown in Fig. 2, existing methods [14]–[16] that rotate the active camera to fixate on more map points that are beneficial for tracking may fail in some VT&R cases because they do not consider the feature identifiability [25], which refers to the ability of the feature detector to identify a 3D map point. While the robot is moving forward in the direction indicated by the arrows (see Fig. 2), existing view planning methods mostly focus the active camera on the regions dense with map points. In many situations, these map points targeted by the active camera are triangulated by earlier keyframes taken from viewpoints significantly different from the current one, making them unidentifiable by the feature algorithms due to their substantially different visual appearances. To address this, we have designed an active camera-based VT&R system featuring an innovative active view planning method that accounts for the view angles of map points. Our FLAF-based active view planning is focal line-centric, as its direction dictates the angles of the active camera.

In this paper we present a visual navigation system with the PTU and a novel active view planning method for feature-based VT&R. The contributions of our work are summarized as follows: (1) We combine VSLAM, motion control in repeat, and feature-based active view planning to overcome the low-texture problem. To the best of our knowledge, this is the first demonstration of VT&R system coupled with active view planning. (2) We propose an online focal line and feature (FLAF)-constrained active view planning method that rewards the camera orientations that observe more feature identifiable map points at their mean-view directions and is suitable for both phases of VT&R.

## II. RELATED WORK

Our active VT&R is based on VSLAM system tightly coupled with active view planning for tracking failure avoidance.

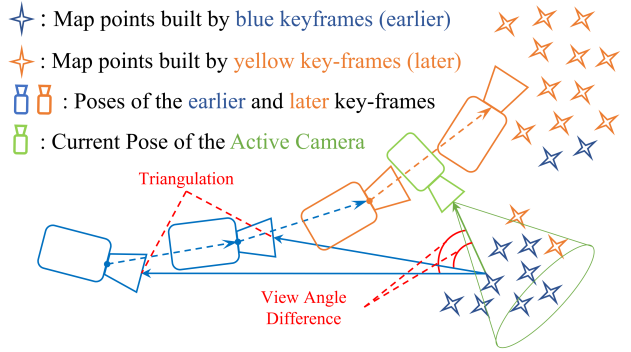


Fig. 2. This is a failure case of existing methods considering only the quantity and distance of map points to the camera center. The keyframes are selected by the VSLAM system in the teach phase. Although the blue points are denser and closer to the camera, they were triangulated from significantly different viewpoints in earlier keyframes, making them difficult to detect from the current viewpoint.

### A. Visual Teach and Repeat

The classical work of VT&R [1] using a feature-based stereo VSLAM was later developed as VT&R2 [2], which utilizes multiple taught experiences to address environmental appearance change. Despite the significant progress, this series of works all suffer from the tracking failure caused by low-texture regions [12] as they all rely on fixed cameras and feature-based VSLAM. Based on the well-established VT&R2 [2], Warren et al. [17] build a gimbal-stabilized VT&R system in which the gimbal is passively utilized to stabilize the camera or manually steered to avoid degeneracy in the teach phase. In the repeat phase, the camera actively rotates to the nearest keyframe in the taught graph. Although this work justified the necessity of an active camera in VT&R, the gimbal is manually steered in the teach phase instead of autonomous operation. Previous works designed various active view planning methods [14]–[17] for active camera-based VSLAM. However, the recently proposed uncertainty-driven view planning (UDVP) [16] that rotates the camera toward more nearby map points easily fails in the repeat phase for it ignores the affine change of features [10] (Fig. 2). To solve these problems, we implement the same autonomous view planning method (FLAF) in both phases of VT&R.

Faced with the aforementioned tracking failure and occlusion, Mattamala et al. [13] designed a VT&R system allowing the quadruped to switch between multiple cameras set on different positions of the robot. However, each one among the cameras faces the same problem of tracking failure. Every camera builds several sub-maps where completion and consistency are difficult to guarantee in sub-map merging without well dealing with the challenging views. Our proposed active VSLAM can help each one of the multiple cameras in [13] to improve the performance of its system. In the meanwhile, our VT&R system is more natural and compact to use fewer computing resources.

### B. Visual Simultaneous Localization and Mapping

Our VT&R system consists of a 3D reconstruction module for the mobile robot to remember a traversed path. In the teach

phase, the robot learns the landmarks in feature-based VSLAM. With the input of an image set that shares observations of the environment, the task of estimating camera motions and a geometrical reconstruction is called Structure From Motion (SfM) [18]. For a mobile robot with a moving video camera, a system that performs SfM for every image as it is captured is called real-time SfM or VSLAM. Specifically, our proposed active view planning method is designed according to the local map built by VSLAM systems [9].

The most popular implementations of VSLAM [7]–[9] follow the principle of aligning the current image to the already-built map for camera localization. The data association between current frame and keyframes and bundle adjustment (BA) are conducted locally and globally to obtain a consistent map [19]. To use time-consuming bundle adjustment in SLAM for optimizing a consistent map, a hierarchical optimization strategy is proposed with the concept of window and local bundle adjustment [20].

In [9], a sophisticated local map is designed to align the current frame and implement the local BA. Motion estimation by aligning the current image to the local map is called local map tracking [7]. Deng [12] et al. identify a particular tracking failure caused by the incapability of associating enough features. In [12] the authors also indicate that the possibility of tracking failure approximates zero if the associated map points is more than a level.

### C. Active View Planning for VSLAM

Seminal work of active view planning for VSLAM is [15], in which Davison et al. indicates the solution of active vision in navigation is using serial views on a succession of features for stable localization and deciding the time to explore new features. Following this idea, [14] proposes to observe the unexplored regions and reset the active camera if features are not enough for localization. However, this strategy doesn't guarantee an accurate localization because the view direction same to the initial one doesn't capture the same initial image as the robot is moving.

In active camera-based VSLAM, the primary problem before the exploration of new features is trying its best to maintain a stable and accurate localization [15]. In [16] the authors propose the UDVP method to measure the quality of the camera angles with respect to every map point. This UDVP model shows fine performance in capturing more existing map points in the Field of View (FoV) of the camera. However, it (shown in Fig. 2) doesn't consider the feature identifiability in the repeat phase which results in tracking failure by looking at unrecognizable map points. Our FLAF method uses the observation model shown in Fig. 3, which utilizes the angle between the camera focal line and the line of sight to a map point to make the camera capture more built map points. In the meanwhile, the angle between the imaging light path of the point and the normal line of the map point is measured to qualify the feature identifiability.

The idea to consider both the angles of  $\alpha_1$  and  $\alpha_2$  shown in Fig. 3 was first described in the VSLAM system of [9]

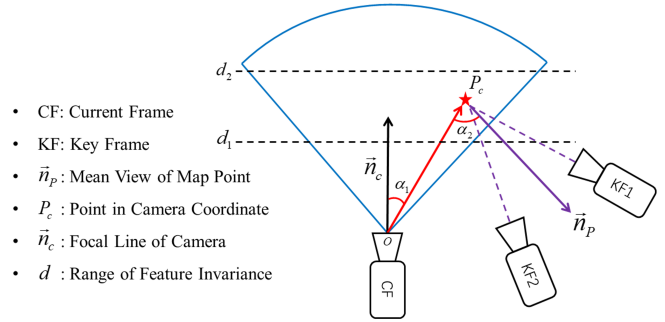


Fig. 3. The observation model of FLAF is used to evaluate the camera pose relative to a map point (3D coordinate). For each pair of PTU angles, the scores of all map points in the local map are summed to assess the view direction. In this model,  $d_1$  and  $d_2$  represent the invariant distance range of a feature point, which constrains the distance between the map point and the optical center. The angle  $\alpha_1$  denotes the angle between the line of sight to the map point and the current camera focal line, while  $\alpha_2$  represents the angle between the line of sight to the point and its mean view line as captured by multiple keyframes. These three metrics are combined to evaluate the camera poses with respect to the local map, determining the optimal PTU angles.

for feature selection, which serves as the foundation for our system. This strategy is also utilized in the active SLAM method presented in [12], which employs a fixed camera for both navigation and exploration. The model in [12] defines specific ranges of distance and  $\alpha_2$  to screen map points within the camera's frustum. The "FLAF without scoring" method in our comparison experiments can be seen as an implementation of active VT&R using the model from [12], despite the differences in the robot and task. It is noteworthy that Mostegel et al. [25] identified several metrics for feature recognition and validated the effectiveness of using a cosine function to measure the feature recognition probability, which indicates the likelihood of feature identification from different view angles.

## III. APPROACH

We build our VT&R system on the active camera-based VSLAM framework shown in Fig. 4, which integrates ORB-SLAM2 [9] and our FLAF-constrained active view planning. Our method for active camera-based path following is similar to that described in [17], which resolves the robot poses from camera localization and PTU angles as the input of VT&R.

To increase the number of map points in the central area of the FoV, we designed a scoring function (Eq. (3)) based on  $\cos(\alpha_1)$  (see Fig. 3) to rotate the camera toward regions dense with map points. As the UDVP model [16] uses a sigmoid function of  $\alpha_1$ , we apply a cosine function to reduce the computational cost. By adding up the scores of all map points within the FoV, each one of them contributes to the total score of this PTU sample. Map points with smaller  $\alpha_1$  values receive higher scores, which encourages the clustering of map points in the central area of the FoV. Consequently, samples of the active camera that capture more map points with smaller  $\alpha_1$  in their FoV achieve higher scores.

Another goal of our design is to score the map points with good feature identifiability relative to the samples of PTU angles. Feature identifiability refers to the ability of the feature

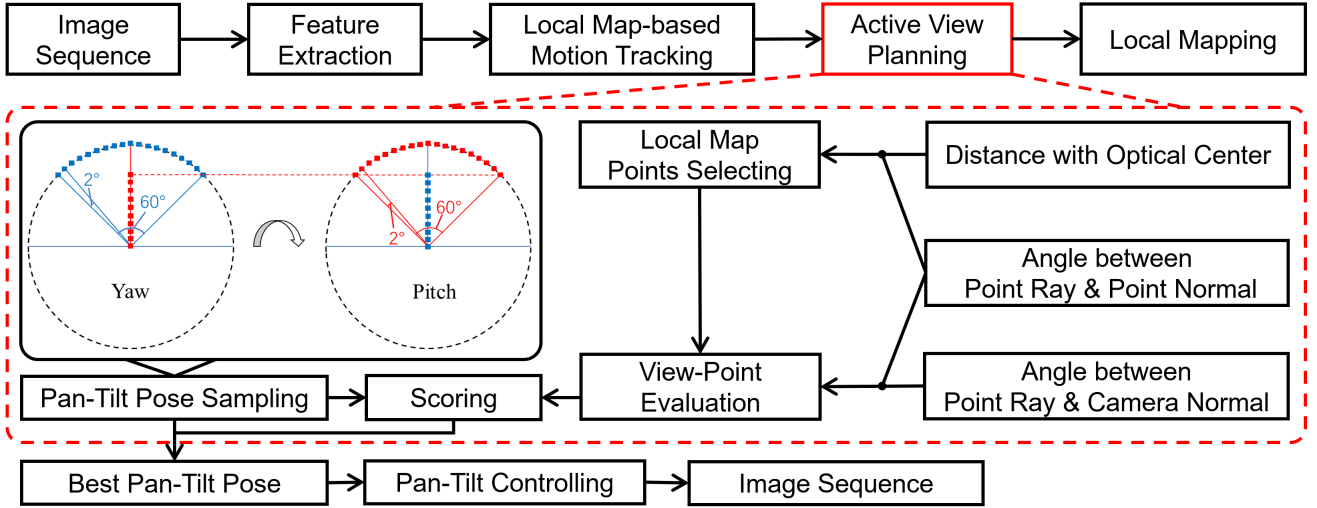


Fig. 4. This is the framework of our active camera-based VSLAM system, which serves as the foundation for the active VT&R system. Our active view planning module is integrated between the local map tracking module and the local mapping module in the passive VSLAM system. The PTU angles in the range of  $60^\circ$  for both yaw angle and pitch angle are sampled with a set interval of  $2^\circ$  and evaluated by our FLAF-constrained view planner. The pan-tilt sample with the highest score, as determined by FLAF, is sent to the PTU control module to adjust the camera direction accordingly.

detector to recognize the map point from a specific position and orientation. With the path map built, the VT&R system can determine the existence of a map point at a 3D coordinate. But if the robot rotates the camera toward this map point from an arbitrary position, there is a probability [25] that this map point may not be detected in the current image due to affine changes [10]. We assume the keyframes that observe the same map point define a view distribution within which this map point can be identified. The mean viewing direction is considered the normal of the map point, around which the view distribution is defined. This definition of the map point normal was also used in [9], [12]. Mostegel et al. [25] justified using  $\cos \alpha_2$  as the metric of the probability of feature identification to account for the observation of a feature from different viewpoints and view angles. Our scoring function,  $\cos(\alpha_1) \cdot \cos(\alpha_2)$ , multiplies two cosine functions to prioritize map points that score highly on both metrics.

#### A. VSLAM with Active Camera

In the classical feature-based VSLAM [9], on which we build our active camera-based SLAM system, the next frame is passively decided by the trajectory of the robot. To avoid low-texture views, we make passive VSLAM tightly coupled with a feature-based active view planning module. Specifically, we insert (Fig. 4) the active view planning module between the local map tracking and the local mapping as they are separated into different threads in implementation.

While the mobile robot is moving along a path, images with equally spaced timestamps are sequentially captured by the moving camera and sent to the VSLAM system. For every input image  $\mathbf{I}_k : \mathbb{R}^2 \rightarrow \mathbb{R}$ , ORB features [21] are extracted and sent to the local-map tracking module, in which features are aligned with the local map to estimate current camera pose  $\mathbf{X}_{k,w} \in \text{SE}(3)$  in world coordinate. This process of computing a camera pose according to the local map is called local map tracking. If enough new features are found, this frame is

decided as a keyframe and these features are triangulated into the map based on data association between local keyframes. This process of projecting new keyframes and features into the map space (world coordinate) is called local mapping.

A local map including a network of keyframes  $\{\mathbf{F}_i\}$  connected according to feature matching and their associated map points  $\{\mathbf{P}_j^i | \mathbf{P}_j^i \in \mathbb{R}^3, j = 0, 1, 2, \dots, m_i\}$  are denoted with:

$$\mathcal{M}_l = \{\mathbf{P}_0^i, \mathbf{P}_1^i, \dots, \mathbf{P}_{m_i}^i, \mathbf{F}_i | i = 0, 1, 2, \dots, n_i\} \quad (1)$$

where  $m_i$  is the quantity of the map points associated with the  $i$ -th keyframe and  $n_i$  is the quantity of the keyframes in the local map. A map point only refers to a 3D coordinate in map space, but its descriptor can be computed from the keyframe by which the point is triangulated. According to the descriptor matching, keyframes share observations with  $\mathbf{I}$  to make up the local map with their associated map points.

For any  $\mathbf{P}_j^i$  in  $\mathcal{M}_l$  that is within the visible frustum of the current camera pose, if it can be matched with an ORB feature at  $\mathbf{p}_j^i \in \mathbb{R}^2$  on  $\mathbf{I}_k$ , it is reprojected onto the  $\mathbf{I}_k$  by pinhole camera model  $\pi : \mathbb{R}^3 \rightarrow \mathbb{R}^2$  and get the reprojected coordinate  $\pi(\mathbf{P}_j^i) \in \mathbb{R}^2$ . The reprojection error as in Eq. (2) is applied for optimizations in VSLAM:

$$\mathbf{e}_{i,j} = \mathbf{p}_j^i - \pi(\mathbf{P}_j^i) \quad (2)$$

We use a set  $\mathcal{S} = \{\mathbf{P}_j^i | \mathbf{P}_j^i \text{ can be identified by } \mathbf{I}_k\}$  to represent the map points in  $\mathcal{M}_l$  that can be identified by the current view. Then local map tracking is conducted by minimizing the cost function [9]:

$$\mathbf{X}_k^* = \arg \min_{\mathbf{X}_k} \sum_{i,j, \mathbf{P}_j^i \in \mathcal{S}} \mathbf{e}_{i,j}^\top \Omega_{i,j}^{-1} \mathbf{e}_{i,j} \quad (3)$$

where  $\mathbf{X}_k^* \in \text{SE}(3)$  represents the pose estimation of  $\mathbf{I}_k$ .

After local map tracking, we have the local map and current camera pose needed in active view planning. Based on the local map and current camera pose, the next best angles of

the PTU can be decided. Thus we achieve using current partial perception results as feedback to control the sensor and image input. According to the results in [12], the pose estimation shown by Equation (3) fails if the magnitude of  $S$  is below a threshold. Therefore, [16] proposes a view planner to increase  $N_S$ . To achieve this by our sampling-based optimization, the pan-tilt angles are sampled as  $\mathbf{q} = (pan, tilt)$  and transformed into  $\mathbf{T}_{pt}(\mathbf{q}) \in SE(3)$  to obtain the corresponding sample of camera pose  $\mathbf{X}'_k$ , which is directly evaluated:

$$\mathbf{X}'_k = \mathbf{T}_{pt}(\mathbf{q}) * \mathbf{X}_k \quad (4)$$

while the robot is moving along a path, the PTU samples are evaluated by view planners at a set frequency, and the best one is sent to the PTU to rotate the active camera. During the simultaneous movements of the PTU and the robot, the images input to the VSLAM are decided by the PTU angles and the robot trajectory, while the PTU angles are decided by the robot trajectory and the local map of the VSLAM system.

### B. Active View Planning for Feature-based VT&R

We use Eq. (5) to represent the magnitude of map points within the visible frustum of the camera that can be matched with an ORB feature in  $\mathbf{I}_k$ :

$$N_S = f(\mathbf{X}_k, \mathbf{M}_l) \quad (5)$$

Eq. (5) indicates that  $N_S$  is a function of the current camera pose and the local map. Using the UDVP observation model [16], we control the active camera to see more and closer map points. Given a PTU sample, the UDVP [16] model scores map points with a smaller distance to the camera center and a smaller view angle between the line of sight to them and the camera's focal line. Thus  $N_S = f(\mathbf{X}_w)$  is increased and tracking failure probability is decreased compared to passive VSLAM. This effect can be represented by the inequality:

$$f(\mathbf{T}_{pt}\mathbf{X}_k) > f(\mathbf{X}_k) \quad (6)$$

However, in the repeat phase, a complete map of the taught path is built. Although there exist more local map points that are close to the optical center and have a small angle between  $OP$  and  $n_c$  ( $\alpha_1$  shown in Fig. 3), some of them can not be identified by the feature detector due to a big angle between the focal line and mean view angle of the map point. This phenomenon can be summarized as "looking at points visible but not identifiable", which results in a higher failure rate of repeat. To address this, we apply the observation model shown in Fig. 3. One distance and two angles are measured for every PTU sample and map point to support our view planner:

- Scoring the pan-tilt sample that makes the map point in the range of  $(d_1, d_2)$  which is the scale invariance range of the image pyramid.
- Scoring smaller  $\alpha_1(\mathbf{T}_{pt}\mathbf{X}_k, \mathbf{P}_j^i)$  shown in Fig. 3 which refers to the angle between camera's focal line  $n_c$  and ray line  $OP$  of the point.
- Scoring reward smaller  $\alpha_2(\mathbf{X}_k, \mathbf{P}_j^i)$  shown in Fig. 3 which refers to the angle between mean view line  $n_p$  and ray line  $OP$  of the point.

According to these three principles, we evaluate every pan-tilt sample with  $M_l$ . At first, we eliminate the points that have a distance out of the range  $(d_1, d_2)$  or have an angle  $\alpha_2 > 60^\circ$ . The rest of the points in the local map make up a collection denoted  $S_r$ . For every map point  $\mathbf{P}_j^i \in S_r$ , we calculate the score of a pan-tilt sample  $\mathbf{q}$  and optimize it by:

$$\mathbf{q}^* = \arg \max_{\mathbf{q}} \sum_{i,j, \mathbf{P}_j^i \in S_r} \cos(\alpha_1)\cos(\alpha_2) \quad (7)$$

The maximum of the cosine functions is achieved when the angle is 0, which indicates that the best view angle is obtained when the focal line of the camera and the mean view angle of the map point overlap.

### C. Path Learning and Tracking with Active Camera

After Teaching, a complete map consisting of plenty of 3D map points and a graph of keyframes are saved with corresponding PTU angles read from the angle encoder. The keyframes with timestamps, poses, and PTU samples contain trajectory information of the active camera and the robot. Then the robot trajectory is computed from PTU samples and camera trajectory by inverse operation of Equation (8):

$$\mathbf{X}_k = \mathbf{T}_{pt}^\top \mathbf{X}'_k \quad (8)$$

Once the repeat begins, the previously taught feature map is loaded, and the PnP algorithm [22] is executed to determine the initial camera pose. The active camera-based VSLAM, as shown in Fig. 2, is then performed to compute the current pose  $\mathbf{X}_{k,w}$ . Following this, we search for the closest keyframe pose  $\mathbf{X}_{r,w} \in SE(3)$  ahead of the current localization. Finally, the pose error between  $\mathbf{X}_{k,w}$  and  $\mathbf{X}_{r,w}$  is processed by a PD controller [23], denoted as  $C_{pd}$ , to calculate the current velocity  $\phi_k$ :

$$\phi_k = C_{pd}(\mathbf{X}_{r,w} - \mathbf{X}_{k,w}) \quad (9)$$

To expedite the reference keyframe search, we define a search window centered on the last reference keyframe, with a fixed width of 10.

## IV. EXPERIMENTS AND DISCUSSION

In both phases of VT&R, the active camera operates automatically according to current perception. During the teaching phase, the robot follows a human-guided path and learns the path automatically using the active camera-based VSLAM. Before the repeating, the robot is placed anywhere near the taught path with a similar orientation to the taught one. Once the repeating begins, the robot autonomously runs along the taught path, adjusting the camera orientation as needed.

The main purpose of our experiments is to demonstrate the repeatable and successful VT&R on the challenging paths with our system. As the trajectory errors of repeating are all acceptable, we emphasize the completion and success rate (CR and SR) as the key results, indicating that only our FLAF-based Active VT&R can complete all four paths at a high SR. Notably, the UDVP-based active VT&R consistently fails at the same location across multiple repetitions.

TABLE I  
COMPARISON BETWEEN PASSIVE VT&R AND ACTIVE VT&R WITH DIFFERENT VIEW PLANNING METHODS

Paths	Metrics	Passive VT&R	UDVP-based Active [16]	FLAF without Scoring [12]	FLAF-based Active (Ours)
Path1(15.08m)	CR(%)	94.36(14.23m)	62.08(9.362m)	72.88(10.99m)	<b>100(15.08m)</b>
	Time(s)	-	0.2036	0.1742	0.2976
	AP-RMSE(m)	0.4992	0.3772	0.2324	0.5333
Path2(19.34m)	CR(%)	100(19.43m)	65.20(12.61m)	87.8(16.99m)	<b>100(19.52m)</b>
	Time(s)	-	0.1973	0.1631	0.3015
	AP-RMSE(m)	0.3573	0.5171	0.4326	0.3058
Path3(29.906)	CR(%)	✘	78.98(23.62)	93.06(27.83)	<b>100(39.08)</b>
	Time(s)	-	0.2365	0.1784	0.3219
	AP-RMSE	-	0.7700	0.9301	1.185
Path4(19.391)	CR(%)	✘	62.11(12.04)	52.77(10.232)	<b>91.27(17.69)</b>
	Time(s)	-	0.3076	0.3394	0.5089
	AP-RMSE	-	0.5085	0.4929	0.6265

All the data in Table I are the average results of 10 repeated experiments. “✘” indicates failures in the teaching phase. The AP-RMSE data of Paths 3 and 4 are relative and lack a definite scale because the ground truths are derived using SfM with images captured by a monocular camera. “CR” means the average completion rate in the repeat stage of VT&R. “Time” means the average time used by the sampling-based view planner.

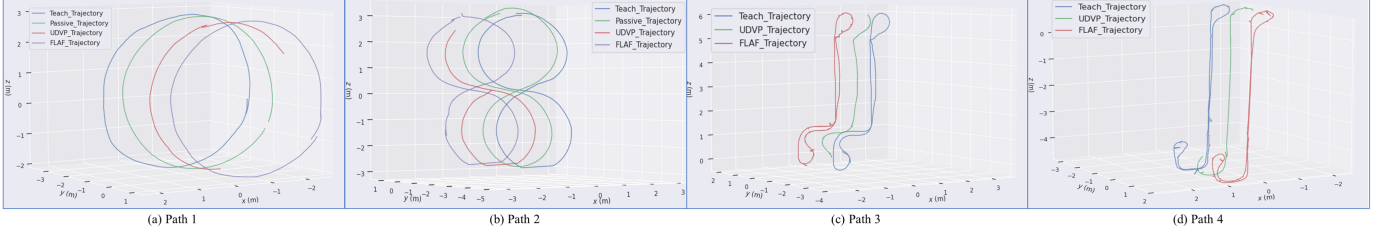


Fig. 5. Trajectories of passive VT&R and active VT&R using different view planning methods are shown. Offsets on the Y-Axis are manually added to separate the overlapping teaching and repeating trajectories for better visualization. The teaching trajectories for Path 1 and Path 2 were obtained via “motion capture” as ground truth, while those for Paths 3 and Path 4 were derived using SfM. Our FLAF-based active VT&R system demonstrates the highest completion rate (CR) across all three paths and can reliably navigate all four paths over multiple loops without failure.

TABLE II  
SUCCESS RATE (SR) ANALYSIS OF THE VT&R SYSTEM IN DIFFERENT VIEW PLANNING METHODS.

Methods	Path1(15.1m)	Path2(19.3m)	Path3(29.9m)	Path4(29.9m)
Passive VT&R	100%	100%	✘	✘
UDVP-based Active	46.7%	13.3%	20%	0%
FLAF without Scoring	73.3%	66.7%	53.3%	33.3%
<b>FLAF-based Active</b>	<b>100%</b>	<b>100%</b>	<b>100%</b>	<b>73.3%</b>

“SR” indicates the success rate of completing the entire path in the repeat phase. The SR data in Table II are the results of 15 repeated experiments. “✘” indicates failure in the teach phase.

We compared our FLAF-based active view planning against three other methods: Passive VT&R, UDVP-based active VT&R, and FLAF without scoring-based active VT&R. Passive VT&R is achieved on our VT&R system without incorporating active view planning. The UDVP-based active VT&R reproduced the observation model proposed in [16] with our VT&R framework. The comparison with “FLAF without scoring” serves as an ablation study, illustrating the impact of our scoring mechanism as described by equation (7). FLAF without scoring-based active VT&R can also be seen as an active VT&R with the model depicted in [12].

### A. Implementation and Experimental Setup

As shown in Figure 1(d), we fix an Intel Realsense D435 camera on an I-Quotient-Robotics PTU to make up our active camera, which is mounted on a Clearpath-Jackal robot. Our active VT&R system runs in real-time on a notebook with an Intel i7 (2.3GHz) CPU and responds to the images exactly at the frame rate of 20Hz.

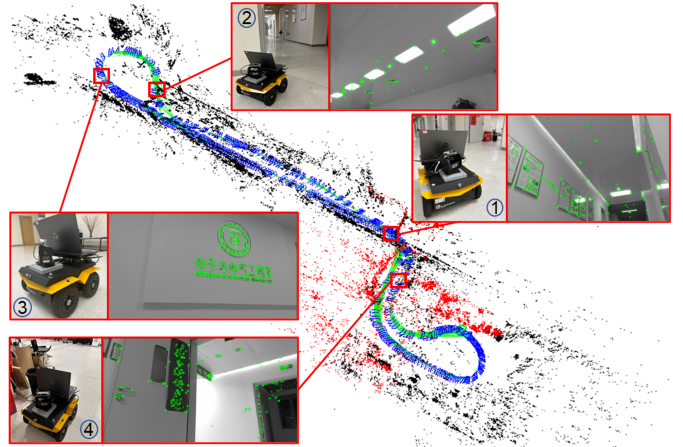


Fig. 6. Feature map of path 3 built by our active SLAM and robot views in repeat phase at challenging locations.

Experiments are performed on four paths to evaluate our active view planning method and VT&R system. The first two paths are in the effective range of the motion capture device in the Shenzhen Key Laboratory of Robotics and Computer Vision. Paths 3 and 4 respectively lead the robot from inside the laboratory to a space out of the laboratory and finally back to the start. All the data in Table I are the average results of 10 repeated experiments. The trajectories shown in Fig. 5 and the plots shown in Fig. 7 are a representative selection, considering that the previous methods consistently fail in the same situation. In Fig. 6, we demonstrate the process during

which our active VT&R system overcomes the low-texture problem on path 3 that connects different rooms.

Ground truths of paths one and two are obtained from motion capture in the teaching phase. The ground truth of Path 3 is built by SfM, as there is no motion capture outside the laboratory. The visual repeating trajectories of all methods are compared with the ground truths and painted in Fig. 5. In Table I, the CR data shown indicates the VT&R completion rate of this view planning method, and the time data indicates the mean time used for the view planning methods implemented by sampling-based optimization. The efficacy of VSLAM is decreased by the relatively low speed of view planning compared to the SLAM speed of 20-30Hz. The translational RMSE of trajectories is computed using evo [24] by comparing the repeat trajectory with the taught one based on timestamps, resulting in greater error than physical truth. The trajectory consistencies between repeat and teach shown in Fig. 4 are all acceptable for T&R.

On paths 1 and 2, we demonstrate the efficacy of our VT&R system in both an active and a passive way. On paths 3 (Fig. 6) and 4, we show challenging cases with low-texture regions where passive VT&R fails and active VT&R succeeds. Additionally, our FLAF model is verified on all four paths to outperform the existing UDVP in repeating a complete path. FLAF without scoring refers to counting the map points in a range defined by FLAF instead of grading the points by the product of the cosine functions shown in Equation (7).

### B. Tracking Failure Avoidance Validation

As in Table I and Fig. 5, the passive VT&R achieves a stable and accurate performance on the first two paths but fails in the teaching phase on paths 3 and 4. The few low-texture regions on path one and two are avoided by a considerable human guide. Our active VT&R system with three view planner succeeds in the teaching phase on all 4 paths.

Fig. 6 demonstrates the situations where low-texture regions are overcome by our active VT&R with an active camera that automatically captures informative regions to maintain a stable localization. At position 1, the active camera automatically looks at the poster in the upper left to avoid the white wall. At position 2, the active camera looks up at the ceiling to maintain the localization relying on the square lamps. The robot looks toward the upper right at position 3 to focus on the logo while passing through a low-texture corner. Finally, at position 4, the robot looks toward the upper left at the scroll on the door for abundant features.

### C. Active View Planning Method Comparison

Active SLAM with different observation models typically succeeds in the teaching phase on all 4 paths. The active camera-based VSLAM has no choice but to see the just mapped points while there are no more feature points triangulated. However, in the repeat phase, existing methods such as UDVP [16] ignore the identifiability of the points by feature detector. Some of the map points (3D coordinates) cannot be

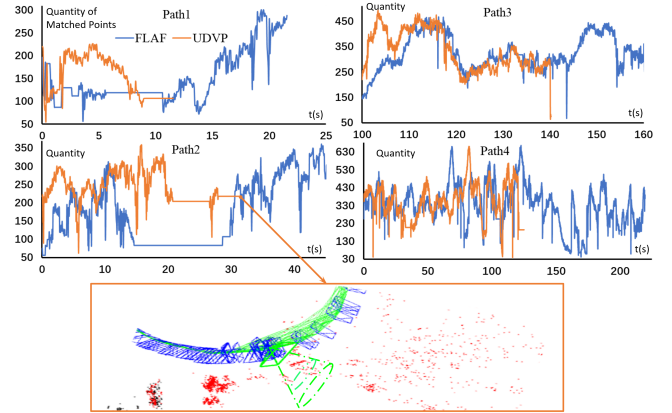


Fig. 7. Number of matched points in local map tracking with respect to time. The bottom shows the failure case of the UDVP method on path 2 shown in a feature map. The green square represents the current pose of the camera.

identified by VSLAM from a large view angle compared with the view direction in which they were triangulated.

Our FLAF-constrained active view planning outperforms the UDVP method in repeating complete paths because it accounts for the affine change of feature points. The normal line of the map point ( $n_p$ ), shown in Fig. 3, limits the orientation of the active camera in the view angle-invariant range of the feature. As seen in Table I, our method repeats more complete trajectories across all paths, especially in challenging scenarios. Although UDVP achieves more accurate path tracking on path 3, the trajectory errors on all paths by all view planners are negligible for VT&R. Part of the AP-RMSE arises from time-wise point-to-point comparisons, which are challenging to execute precisely. To address this, we modified the timestamps to be uniformly consistent over the same time duration. The trajectories shown in Fig. 5 further confirm that the repeat consistencies with different methods are all pretty good, as the repeated trajectories align well with the taught ones.

### D. Map Points Association Validation

In [12], the authors present a line graph illustrating the relationship between the probability of the tracking failure and the number of observed feature points. Their results [12] indicate that the likelihood of the tracking failure approaches zero when the number of associated map points exceeds a certain threshold. From the perspective of our work, the specific failure is caused by choosing the wrong orientation of the active camera relative to the local map. To further investigate, we applied the analysis method proposed by [12] to examine the state of map point association during the repeating phase.

As shown in Fig. 7, we recorded the number of inlier points successfully matched during local map tracking and plotted line graphs comparing the performance of the two methods across all test paths. On paths 1 and 2, the active camera-based VSLAM with FLAF initially matched fewer points than the UDVP-based system. However, after an initial reduction of matched points, the UDVP-based method fails to maintain tracking, while the FLAF-based method continues to provide

stable localization and an increasing number of matches. This phenomenon suggests that, once the inlier number of the tracked map points reaches the threshold, the sheer number of map points becomes less critical for stable localization. The bottom of Fig. 7 also illustrates how the UDVP method directs the active camera toward regions with more local map points, without accounting for the feature identifiability. Although many points may fall within the camera's FoV, they may not be recognized or matched by the feature extractor due to the ignorance of the affine changes.

On paths 3 and 4, the active visual repeat with both the FLAF and UDVP view planners tracks a similar quantity of map points. However, our FLAF-based method successfully recovers localization after a challenging decline in tracked points, where the UDVP-based approach fails. Even in cases of temporary tracking loss, the active camera controlled by our view planner was able to orient itself appropriately by executing the instruction before tracking loss, allowing the VSLAM system to recover localization through place recognition and the PnP algorithm.

## V. CONCLUSION

In this research, we present a novel active view planning method for VT&R that addresses the tracking failure caused by the low-texture regions and demonstrates the whole active VT&R. Our experimental results show that our active VT&R successfully overcame the specific failure of passive VT&R and our proposed FLAF-constrained active view planning outperforms existing view planners in completion and success rate of VT&R.

A previous active camera-based VT&R manually steered a gimbal-stabilized camera instead of rotating actively for failure avoidance. Existing active camera-based VSLAM methods did not demonstrate how to integrate their View planners into visual navigation systems. During our tests, the VT&R systems built on these active camera-based VSLAM systems easily failed in the repeat phase without considering the feature-identifiability of the map points. Our proposed focal line and feature (FLAF)-constrained active view planning successfully addressed these failures by considering the view angle difference between the current viewpoint and those at which the map points were triangulated. With our view planner, the active VT&R system successfully finishes all four paths at the highest completion and success rate. Additionally, our point-line plots indicate that the quality of the map points is more important than quantity for stable localization.

However, for each execution of view planning, 900 samples of PTU angles were scored according to thousands of map points in the local map, resulting in a high computational overhead. Despite using OpenMP to speed up the view planners, they operated at less than 5 FPS, which hindered the performance of VSLAM and reduced the success rate of VT&R by preventing accurate path reconstruction. In future work, we will address this limitation by parallelizing the view planning module with the VSLAM system to improve processing speed and overall system performance.

## REFERENCES

- [1] Paul Furgale, and Timothy D Barfoot, "Visual teach and repeat for long-range rover autonomy," *Journal of Field Robotics*, 2010.
- [2] Michael Paton, Kirk MacTavish, Michael Warren, Timothy D Barfoot, "Bridging the appearance gap: Multi-experience localization for long-term visual teach and repeat." In *IEEE/RSJ Int. Conf. on Intell. Robots and Systems*, 2016.
- [3] L. Peterson, D. Austin, and D. Kragic, "High-level control of a mobile manipulator for door opening," In *IEEE/RSJ Int. Conf. on Intell. Robots and Systems*, 2000.
- [4] Mohit Mehndiratta and Erdal Kayacan, "A constrained instantaneous learning approach for aerial package delivery robots: onboard implementation and experimental results," *Autonomous Robots*, 2019.
- [5] Guillaume Bresson, Zayed Alsayed, Li Yu, and Sébastien Glaser, "Simultaneous Localization and Mapping: A Survey of Current Trends in Autonomous Driving," *IEEE Trans. Intell. Vehicles*, 2017.
- [6] H Ye, G Chen, W Chen, L He, Y Guan, and H Zhang, "Mapping While Following: 2D LiDAR SLAM in Indoor Dynamic Environments with a Person Tracker," In *IEEE Int. Conf. on Robot. and Biomimetics*, 2021.
- [7] Jakob Engel, Vladlen Koltun, and Daniel Cremers. "Direct sparse odometry." *IEEE Trans. Pattern Anal. Mach. Intell.*, 2017.
- [8] Christian Forster, Matia Pizzoli, and Davide Scaramuzza. "SVO: Fast semi-direct monocular visual odometry." In *IEEE Int. Conf. on Robotics and Automation*, 2014.
- [9] R. Mur-Artal, J. M. M. Montiel, and J. D. Tardos, "Orb-slam: a versatile and accurate monocular slam system," *IEEE Trans. Robotics*, 2015.
- [10] David G Lowe. "Distinctive image features from scale-invariant keypoints." *International Journal of Computer Vision*, 2004.
- [11] Seyed Abbas Sadat, Kyle Chutskoff, Damir Jungic, Jens Wawerla and Richard Vaughan, "Feature-Rich Path Planning for Robust Navigation of MAVs with Mono-SLAM," In *IEEE Int. Conf. on Robotics and Automation*, 2014.
- [12] Xinke Deng, Zixu Zhang, Avishai Sintov, Jing Huang, and Timothy Bretl, "Feature-constrained Active VSLAM for Mobile Robot Navigation," In *IEEE Int. Conf. on Robotics and Automation*, 2018.
- [13] Matias Mattamala, Milad Ramezani, Marco Camurri, and Maurice Fallon. "Learning Camera Performance Models for Active Multi-camera Visual Teach and Repeat." In *IEEE Int. Conf. Robotics and Automation*, 2021.
- [14] Simone Frintrop, and Patric Jensfelt. "Attentional Landmarks and Active Gaze Control for VSLAM." *IEEE Trans. Robotics*, 2008.
- [15] Andrew J. Davison and David W. Murray. "Mobile Robot Localisation using Active Vision." In *European Conf. Computer Vision*, 1998.
- [16] Xu-Yang Dai, Qing-Hao Meng, and Sheng Jin. "Uncertainty-driven Active View Planning in Feature-based Monocular vSLAM." *Applied Soft Computing*, 2021.
- [17] Michael Warren, Angela P. Schoellig, and Timothy D. Barfoot. "Level-headed: Evaluating Gimbal-stabilised Visual Teach and Repeat for Improved Localisation performance." In *IEEE Int. Conf. Robotics and Automation*, 2018.
- [18] Hauke Strasdat, José MM Montiel, and Andrew J. Davison. "VSLAM: why filter?" *Image and Vision Computing*, 2012.
- [19] Weinan Chen, Changfei Fu, Lei Zhu, Shing-Yan Loo, and Hong Zhang. "Rumination Meets VSLAM: You Do Not Need to Build All the Submaps in Realtime." *IEEE Trans. Industrial Electronics*, 2023.
- [20] Etienne Mouragnon, Maxime Lhuillier, Michel Dhome, Fabien Dekeyser, and Patrick Sayd. "Real Time Localization and 3D Reconstruction." In *IEEE Int. Conf. Computer Vision and Pattern Recognition*, 2006.
- [21] Ethan Rublee, Vincent Rabaud, Kurt Konolige, and Gary Bradski. "ORB: An efficient alternative to SIFT or SURF." In *IEEE Int. Conf. Computer Vision*, 2011.
- [22] Vincent Lepetit, Francesc Moreno-Noguer, and Pascal Fua. "EPnP: An accurate O(n) Solution to the PnP Problem." *International Journal of Computer Vision*, 2009.
- [23] Weinan Chen, Lei Zhu, Xubin Lin, Li He, Yisheng Guan, and Hong Zhang. "Dynamic Strategy of Keyframe Selection with PD Controller for VSLAM Systems." *IEEE/ASME Trans. Mechatronics*, 2021.
- [24] Michael Grupp. "evo: Python package for the evaluation of odometry and slam." 2017, Available: <https://github.com/MichaelGrupp/evo>.
- [25] Christian Mostegel, Andreas Wendel, and Horst Bischof. "Active Monocular Localization: Towards Autonomous Monocular Exploration for Multirotor MAVs." In *IEEE Int. Conf. Robotics and Automation*, 2014.